Neoplasia • Vol. 9, No. 2, February 2007, pp. 119–127 119

www.neoplasia.com

Target Therapy Using a Small Molecule Inhibitor against Angiogenic Receptors in Pancreatic Cancer[1]

Peter Büchler[*,†], *Howard A. Reber*[*], *Mendel M. Roth*[*], *Mark Shiroishi*[*], *Helmut Friess*[†] *and Oscar J. Hines*[*]

[*]Department of Surgery, UCLA School of Medicine, University of California, Los Angeles, CA 90095-6904, USA; [†]Department of Surgery, University of Heidelberg, Im Neuenheimer Feld, Heidelberg 69120, Germany

Abstract

PURPOSE: **PD173074, a small molecule inhibitor of VEGF-RII and FGF-RI, targets neoangiogenesis and mitogenesis. This study aimed to analyze a single-compound-driven inhibition of FGF and VEGF receptors in pancreatic cancer.** ***EXPERIMENTAL DESIGN:*** **RT-PCR and Western blots were performed to quantify protein expression and phosphorylation. Anchorage dependent and independent growth assays were used to study cell growth. With flow cytometry, cell cycle analysis and apoptosis were studied.** ***In vivo*** **HPAF-II and MIA PaCa-2 cells were xenografted. Animals were treated daily for 10 weeks. Immunohistochemistry was used to quantify microvessel density and apoptosis.** ***RESULTS:*** **Highest levels of FGF-RI were detectable in MIA PaCa-2 cells, lowest in HPAF-II cells. PD173074 inhibited cell growth most prominently in cells expressing high levels of FGF-RI. Cell cycle progression was inhibited by blocking transition in the G_0/G_1 phase, and consequently, apoptosis was increased.** ***In vivo*** **significant inhibition of orthotopic tumor growth was achieved by a combination effect of inhibition of mitogenesis, induction of apoptosis, and reduction of angiogenesis in PD173074-treated animals.** ***CONCLUSIONS:*** **These data highlight VEGF-RII and FGF-RI as therapeutic targets and suggest a potential role for the combined use of tyrosine kinase inhibitors in the management of inoperable pancreatic cancer patients.** *Neoplasia* (2007) **9,** 119–127

Keywords: Angiogenesis, antiangiogenic therapy, pancreatic cancer, tyrosine kinase inhibitors, VEGF receptor.

Introduction

Angiogenesis is an essential physiological process during organ development but is also involved in many pathological circumstances such as diabetic retinopathy, atherosclerosis, cancer growth, and metastasis [1,2]. Pancreatic cancer is the fourth or fifth leading cause of cancer death in western countries, with nearly 32,000 people diagnosed annually and with almost the same number of patients dying from this disease in the United States [3]. Overall, the incidence of pancreatic cancer remains stable in men but, for unknown reasons, is rising in women [3–5]. Apart from a few patients suffering from certain types of hereditary pancreatitis, little is known about risk factors for this disease [6].

The highly aggressive nature of pancreatic cancer remains to be elucidated but could be due to differential expression of growth factors, resulting in high constitutive intrinsic tyrosine kinase activity, which simultaneously stimulates cell proliferation and tumor angiogenesis [7–9]. An increasing awareness of the role of tumor neoangiogenesis in the growth of solid tumors has led to a consensual opinion that abrogated neoangiogenesis may cause tumor growth arrest [10].

Numerous studies have indicated that angiogenesis involves different cytokines, such as vascular endothelial growth factor (VEGF), basic fibroblast growth factor (bFGF), or angiopoietin 1 [11,12]. As of now, it appears that members of the FGF—in particular the VEGF—family are the most potent proteins involved in tumor neoangiogenesis and, in the case of pancreatic cancer, possess an additional mitogenic effect [13]. VEGF and bFGF are overexpressed in pancreatic cancer and accelerate tumor growth [14,15]. The cellular effects of these peptides are mediated by specific cell surface receptors with intrinsic tyrosine kinase activity [16–21]. Disruption of VEGF signaling with neutralizing antibodies or by dominant-negative Flk-1 receptor mutants slows tumor growth. In contrast, suppression of VEGF signaling alone had no effect on tumor growth, suggesting that other angiogenic factors may substitute for VEGF or bFGF [22,23]. This switch might be of particular interest because FGF-RI activation causes activation of mitogen-activated protein kinases, which in turn regulate VEGF gene expression [24–26].

In the present study, we analyzed the preclinical therapeutic potential of a novel small molecule inhibitor, designated PD173074, *in vitro* and *in vivo* using a clinically relevant orthotopic model for pancreatic cancer [27,28]. This small molecule inhibitor has been shown to be a highly selective tyrosine kinase inhibitor for both FGF-RI in lower doses (~ 25 nM) and VEGF-RII signaling in higher doses (~ 100 nM) [27,28] in fibroblasts.

Address all correspondence to: Peter Büchler, MD, Department of General Surgery, Ruprecht-Karls-University of Heidelberg, Im Neuenheimer Feld 110, Heidelberg 69120, Germany.
E-mail: peter.buechler@med.uni-heidelberg.de

[1]This work was supported by the Ronald S. Hirshberg Pancreatic Cancer Research Foundation.
Received 27 September 2006; Revised 8 January 2007; Accepted 9 January 2007.

DOI 10.1593/neo.06616

Because of its antiangiogenic potential in angiogenic tumor model systems, we used this compound in higher doses to simultaneously inhibit FGF-RI and VEGF-RII signaling and to tailor therapy to pancreatic cancer because cancer cells require higher drug doses for growth suppression. We hypothesized that simultaneous blockade of these receptors may not only abrogate angiogenic pathways but also bifunctionally downregulate tumor cell proliferation.

Materials and Methods

Cell Culture

Five human pancreatic cancer cell lines (AsPC-1, Capan-1, HPAF-II, MIA PaCa-2, and PANC-1) were used *in vitro*, and MIA PaCa-2 and HPAF-II were also studied *in vivo* [29–33]. All cancer cell lines were purchased from the American Type Culture Collection (Rockville, MD) and cultured in Dulbecco's modified Eagle's medium or RPMI 1640 medium supplemented with 10% heat-inactivated fetal bovine serum, penicillin G (100 U/ml), and streptomycin (100 μg/ml). Human umbilical vein endothelial cells (HUVECs) were cultured in an endothelial cell growth medium containing an endothelial cell growth supplement (PromoCell GmbH, Heidelberg, Germany). Normal human dermal fibroblasts (NHDFs) were purchased from PromoCell GmbH and cultured in fibroblast growth medium supplemented with insulin (5 μg/ml) and bFGF at a final concentration of 1 ng/ml. All cell culture chemicals were purchased from Life Technology (Rockville, MD). All other chemicals were obtained from Sigma Chemicals (St. Louis, MO), unless otherwise indicated. PD173074 was kindly provided by Parke-Davis (Ann Arbor, MI). The doses of PD173074 tested were 0, 1, 10, and 50 μM, or an equal volume of solvent, which was used as the solvent of PD173074. The doses used in this study were chosen because lower doses used for endothelial growth suppression did not inhibit pancreatic cancer cell growth. All *in vitro* growth studies were performed in 35-mm dishes as a monolayer culture with logarithmically growing cultures.

Cell Number, Viability, and Growth

To determine the cell number, cells were trypsinized and pelleted by centrifugation for 5 minutes at 1500 rpm, resuspended in 10 ml of phosphate-buffered saline (PBS), and counted with an improved Neugebauer hemocytometer. Cell viability was assayed by MTT [3-(4,5-dimethylthiazol-2-yl)-2,5-diphenyltetrazolium bromide] colorimetric assay [34] using a commercially available kit (Boehringer Mannheim, Mannheim, Germany) according to the manufacturer's instructions. Absorbency readings were performed on a 540-nm multiwell spectrophotometer ELISA Reader (Biotek Instruments, Burlington, VT).

Cell Proliferation Assay

For [^{3}H]thymidine incorporation, 1×10^4 to 3×10^4 cells were grown for 2 days in complete cell medium and serum-starved for 24 hours. After serum deprivation, cells were grown in normal cell type–specific medium, and DNA synthesis was measured by adding 5 μCi of [^{3}H]thymidine (APB, Uppsala, Sweden) for 6 hours. Cultures were washed with PBS, fixed with 5% trichloracetic acid (TCA), and lysed in 500 μl of lysis base containing 0.1 N NaOH + 1% sodium dodecyl sulfate (SDS). Afterward, [^{3}H]thymidine incorporation was measured by liquid scintillation counting (Beckman, Fullerton, CA). The assays were performed in triplicate and repeated at least twice.

Cell Cycle Analysis with Flow Cytometry

Samples were analyzed on a FACScan flow cytometer (Becton Dickinson Immunocytometry Systems, San Jose, CA) equipped with a 488-nm argon ion laser. Green fluorescein isothiocyanate (FITC) fluorescence was collected with a 530/30–nm bandpass filter. Orange emission from propidium iodide (PI) was filtered through a 585/42–nm bandpass filter. Emission of 7-amino-actinomycin D (7-AAD) was collected through a 650-nm longpass filter. Photomultiplier tube voltage and spectral compensation were initially set using cells single-stained with either FITC-labeled monoclonal antibody, PI, or 7-AAD alone. FITC and 7-AAD fluorescence data were shown on four-decade log scales. PI fluorescence was collected using linear amplification, in addition to FL-2 (orange fluorescence) height. FL-2 areas (*A*) and width (*W*) were measured to permit doublet discrimination. A low flow rate setting (12 μl/min) was used for sample acquisition to improve the coefficient of variation (% CV) on DNA histograms. A minimum of 7500 events was collected on each sample. Analysis of multivariate data was performed with CELLQuest software (Becton Dickinson Immunocytometry Systems). Cell cycle analysis of DNA histograms was performed with ModFit LT software (Verity Software House, Topsham, ME).

Apoptosis Assays

The amount of apoptotic cells was analyzed with annexin V binding using an Annexin V FLOUS Staining Kit (Boehringer Mannheim). Briefly, cells were washed twice with PBS and then resuspended in 100 μl of annexin V staining solution, which consisted of 20 μl of FITC-conjugated annexin V reagent (20 μg/ml), 20 μl of isotonic PI (50 μg/ml), and 1000 μl of 1 M HEPES buffer (all supplied by the manufacturer). Cells were incubated in staining solution for 10 minutes at 25°C. Following this incubation, 500 μl of binding buffer (supplied by the manufacturer) was added, and cells were analyzed by flow cytometry. Samples were analyzed on a FACScan flow cytometer (Becton Dickinson Immunocytometry Systems) equipped with a 15-nW air-cooled 488-nm argon ion laser. Because positive annexin V staining is seen for apoptotic and necrotic cells, PI was used to differentiate between these two subgroups. Annexin V–positive and PI-positive cells were considered necrotic cells, whereas annexin V–positive and PI-negative cells were counted as apoptotic cells.

Soft Agar Colony-Forming Assay

For anchorage-independent growth assays, a bottom layer of 1 ml of cell type–specific medium containing 0.7% agar (DIFCO, Detroit, MI) and 10% fetal bovine serum was

poured. Then 1×10^4 cells were added in 1 ml of complete culture medium, 0.35% agar, and various concentrations of PD173074. Cells were incubated in cell type–specific culture conditions; after 10 days, MTT reagent, which is exclusively metabolized by living cells, was added at a final concentration of 0.5 mg/ml for vital staining. Colonies with > 20 cells were counted manually.

Immunoprecipitation and Western Blot Analysis

Cells were lysed in radioimmunoprecipitation assay buffer (1× PBS, 1% Nonidet P-40, 0.5% sodium deoxycholate, and 0.1% SDS) with a protein inhibitor (10 μl/ml radioimmunoprecipitation assay buffer of 10 mg/ml phenylmethylsulfonyl fluoride in isopropanol, 30 μl/ml radioimmunoprecipitation assay buffer of aprotinin, and 10 μl/ml radioimmunoprecipitation assay buffer of 100 mmol of sodium orthovanadate). Samples were incubated on ice for 30 minutes and centrifuged at 10,000*g* for 15 minutes. Protein concentrations were determined, and FGF-RI was detected by a specific antibody recognizing the COOH terminus of each of these FGF-RI (1:1000; Santa Cruz Biotechnology, Santa Cruz, CA). Equal amounts of protein were immunoprecipitated with antisera FGF-RI attached to protein A/G plus agarose beads and separated on 8% polyacrylamide gel. Immunoblotting analyses were performed by probing with a monoclonal antiphosphotyrosine (PY99; Santa Cruz Biotechnology) and with FGF-R as control. The effect of FGF-R tyrosine kinase inhibition was also examined in the presence of FGF-1 stimulation (5 ng/ml) for 15 minutes. Similarly, VEGF-RII was immunoprecipitated with an antireceptor antibody, followed by immunoblotting with an antiphosphotyrosine monoclonal antibody.

Tumor Induction in Athymic Nude Mice

Five-week-old male nude mice (BALB/Ca) were used for subcutaneous and orthotopic tumor implantations [35,36]. The experimental protocol was approved by the Chancellor's Animal Research Committee of the University of California (Los Angeles, CA) in accordance with national guidelines for animal care and the use of laboratory animals. The poorly differentiated human pancreatic cancer cell line MIA PaCa-2 and the more differentiated HPAF-II cell line were used for xenograft tumor induction. After subcutaneous tumor formation, one small tumor fragment (~ 1 mm in diameter) was removed from the subcutaneous tumor and transplanted into the tail of the mouse pancreas. To standardize experimental conditions *in vivo*, all 20 animals for each cell line to be tested were transplanted in the same session with tumor pieces from the same subcutaneous tumor and randomly assigned to either the PD173074-treated group ($n = 10$) or the sham-treated group ($n = 10$). After orthotopic tumor transplantation, the mice were inspected daily. The growth rate of the tumor was monitored by abdominal palpation, and tumor volume was determined after the sacrifice of animals using the formula: tumor volume = 1/2(length × width × depth). Metastatic tumor spread was determined macroscopically in all thoracic, abdominal, retroperitoneal, and pelvic organs, and all suspicious lesions were confirmed by microscopic analysis. Metastatic spread was quantified by counting different organs that contained metastatic lesions. Thus, every point in the metastatic score represented a different organ of metastatic tumor spread, as previously described [35]. Ascites volume was measured with a single-channel adjustable 1000-μl laboratory Eppendorf pipette.

Therapeutic Efficiency of PD173074 in Athymic Nude Mice

One week after orthotopic tumor transplantation, treatment was initiated. PD173074 (25 mg/kg per day) was given intraperitoneally in a volume of 0.1 ml in PBS, which also served as control vehicle. Treatment was continued until sacrifice, which was performed when clinical signs of excess tumor burden, such as cachexia or ascites with abdominal distension, became evident or when the tumor has grown larger than 1.5 cm.

Immunohistochemical Labeling for the Quantitation of Microvessel Density (MVD)

Tumors were fixed in 10% buffered formalin, embedded in paraffin, and sectioned (2–4 μm) for hematoxylin–eosin staining or immunohistochemistry. Apoptosis staining was performed using the TUNEL method according to the manufacturer's instructions (Roche Diagnostics, Penzberg, Germany). Labeling of microvessels was performed with rat anti-mouse CD31 (PharMingen, San Diego, CA), followed by biotinylated goat anti-rat antibody (Jackson ImmunoResearch Laboratories, West Grove, PA) and streptavidin-conjugated horseradish peroxidase (DAKO, Carpinteria, CA) using a protocol that has been previously described in detail [36]. Quantification of MVD has been described previously [36–40]. Briefly, MVD was determined using three sections of each xenograft tumor cut from different tumor regions. On each slide, three vascular hot spots were selected by scanning a tumor section at low magnification (×40). Once the vascular hot spot has been defined, a higher magnification was selected to be able to count individual microvessels. Magnifications on the order of ×200 and a field size of 0.25 mm^2 were used [37,39,40]. Thus, quantification of stained vessels was achieved by measuring the highest microvascular density. All measurements were performed by a single pathologist blinded to the sample's identity.

Statistical Analysis

Experiments were repeated at least thrice. Results are expressed as mean ± SE. Statistical significance was determined by Student's *t* test ($P < .05$).

Results

FGF-RI Expression in Pancreatic Cancer Cell Lines

It has previously been reported that the angiogenic system consisting of VEGF and its receptors VEGF-RI and VEGF-RII is activated in human pancreatic cancer growth [7,41]. Therefore, we determined the expression and phosphorylation of FGF-RI. We measured FGF-RI mRNA by reverse transcription–polymerase chain reaction (RT-PCR),

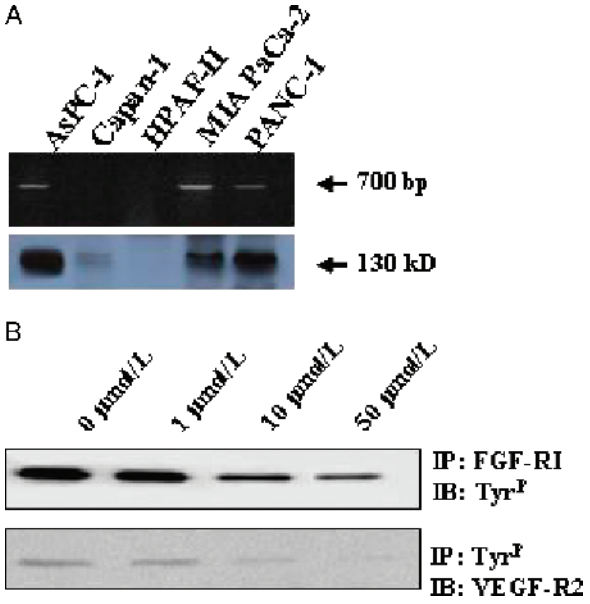

Figure 1. *Expression of FGF-RI in pancreatic cancer cell lines. (A) mRNA was isolated, and RT-PCR was performed. After PCR with specific primers for FGF-RI, the PCR product was separated on a 1% agarose gel (upper panel). The corresponding FGF-RI Western blot analysis is shown below (lower panel). In (B), the effect of PD173074 on FGF-RI and VEGF-RII signaling is shown. AsPC-1 cells were grown for 24 hours in the presence or in the absence of PD173074 and were stimulated for 15 minutes with FGF-1 (50 μg/ml) in the presence of heparin or stimulated with recombinant human VEGF (25 ng/ml). Total cell lysates were immunoprecipitated (IP); subsequently, immunoblotting (IB) was performed with the indicated antibodies.*

and protein expression was quantified by Western blot analysis. FGF-RI mRNA expression was detectable in three of five cell lines (Figure 1*A*). In Western blot analysis, these cell lines also exhibited the expression of FGF-RI protein, whereas cell lines devoid of FGF-RI mRNA did not express relevant protein levels (Figure 1*A*). Whether PD173074 inhibits FGF-RI or VEGF-RII phosphorylation in pancreatic cancer cells was tested in the AsPC-1 cell line. Cell lysates from PD173074-treated cells were subjected to FGF-RI immunoprecipitation, followed by blotting with an antiphosphotyrosine antibody. In the case of VEGF-RII, immunoprecipitation was performed with an antiphosphotyrosine antibody, followed by blotting with VEGF-2 antibody. Although robust FGF-1–mediated and VEGF-mediated phosphorylations were evident in the absence of the small molecule inhibitor PD173074, cells pretreated with PD173074 showed a dose-dependent inhibition of FGF-RI and VEGF-RII phosphorylation (Figure 1*B*). The functional relevance of this observation was further studied in cell proliferation assays measuring DNA synthesis by [^{3}H]thymidine uptake. In this assay, mitogenic response was detectable on stimulation of pancreatic cancer cells with recombinant human VEGF and FGF-1 (Figure 2). The mitogenic response induced by the addition of either of the two cytokines was blocked by increasing doses of PD173074, which in high doses even suppressed the basal cell proliferation rate (Figure 2*B*). The functional relevance of the VEGF-mediated growth stimulation of pancreatic cancer cells has previously been reported [7,8,41].

PD173074 Suppressed Cell Growth

The culture of pancreatic cancer cell lines in the presence of PD173074 resulted in a dose-dependent and time-dependent growth suppression. This finding was detectable in cell counts (Figure 3, *B* and *D*) and was confirmed in MTT assays (Figure 3, *B* and *D*), where a strong time-dependent (Figure 3, *A* and *B*) and dose-dependent (Figure 3, *C* and *D*) growth inhibition was detectable. The IC_{50} dose of pancreatic cancer cell lines was in the range of 2.5 to 15 μM, depending on the individual cancer cell line (data not shown). In comparison, nontransformed normal human cells are more susceptible to PD173074 therapy (50-fold to 100-fold) than are cancer cells. HUVECs and human fibroblast cells showed a marked reduction in cell viability at PD173074 doses of 0.01 to 0.1 μM, as analyzed by MTT assays (Figure 3*E*).

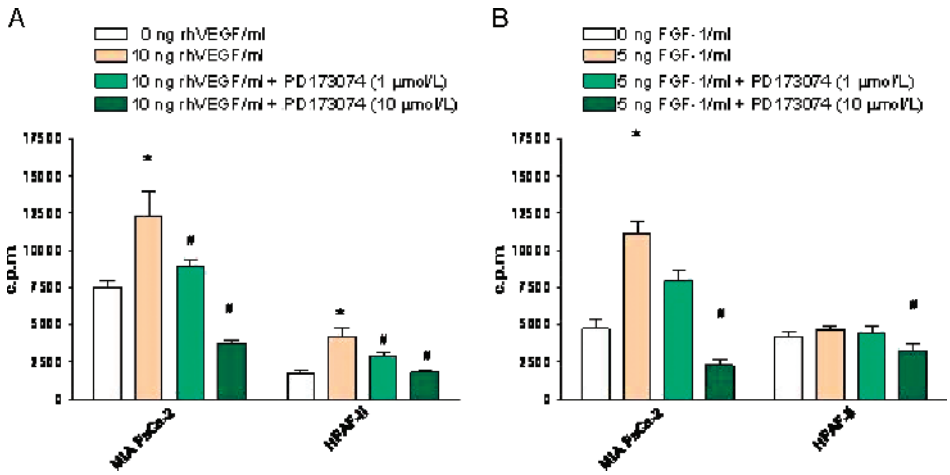

Figure 2. *[^{3}H]thymidine incorporation on FGF-1 and VEGF stimulation of various human pancreatic cancer cell lines. (A) Cells (~ 5×10^4) were grown for 3 days and stimulated with different doses of recombinant human VEGF (1 and 10 ng/ml). In (B), cells were stimulated with recombinant human FGF-1 (0, 1, and 5 ng/ml). The inhibitory effect of PD173074 was tested by adding PD173074, 60 minutes before the addition of growth factors at two different concentrations (1 and 10 μM). After 14 hours of stimulation, cells were pulse-labeled for 6 hours with [^{3}H]thymidine (0.25 μCi/ml). Values represent the mean ± SE of at least three independent experiments. *P < .05, compared with untreated cells. #P < .05, compared with cells stimulated with VEGF or FGF-1.*

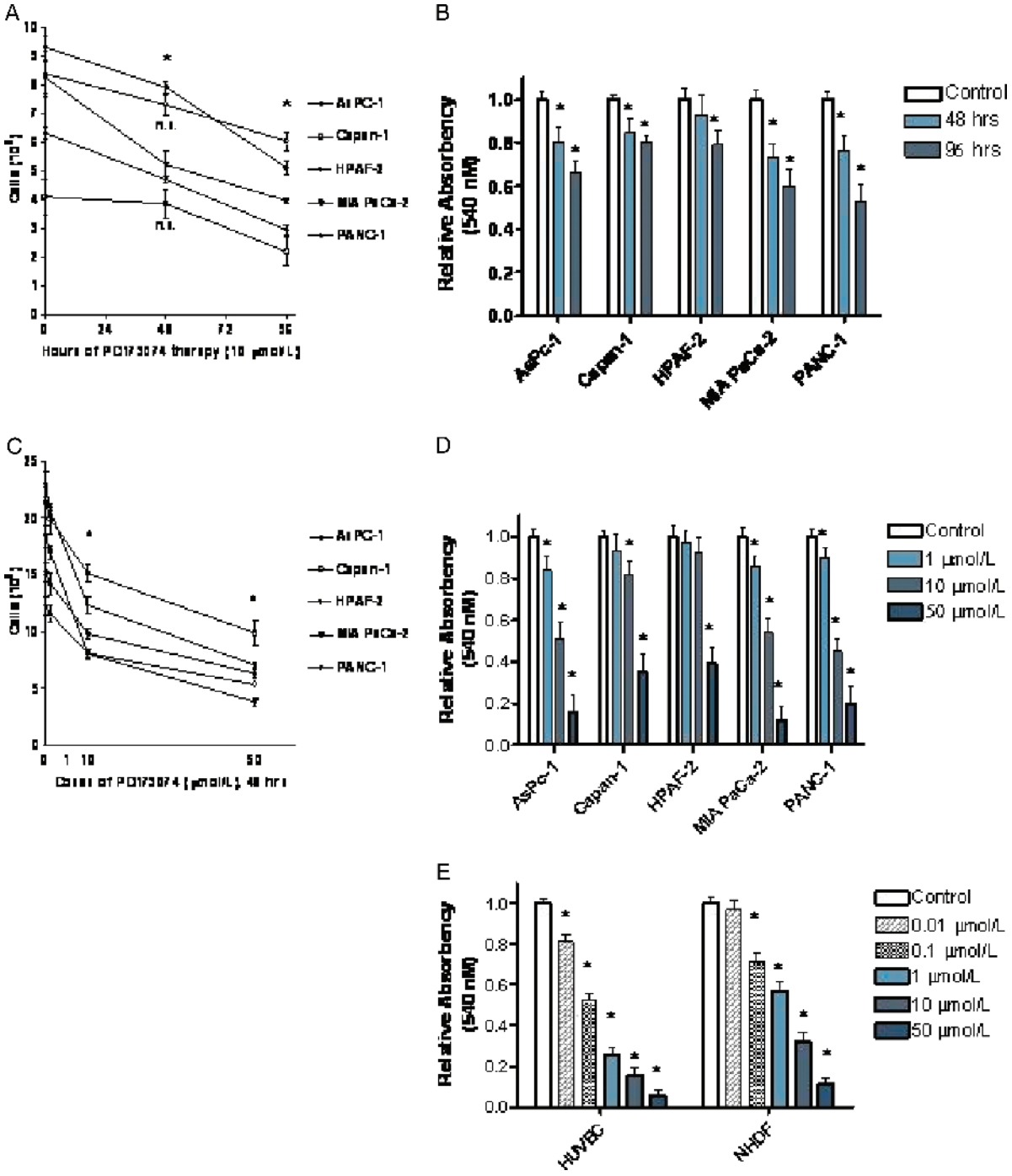

Figure 3. *Dose-dependent and time-dependent effects of PD173074 on cell growth in different human pancreatic cancer cell lines. (A and B) Time-dependent effect of PD173074 (10 μM) on pancreatic cancer cell growth. (A) Cells were grown in complete cell medium for up to 96 hours in the presence of 10 μM PD173074. Cells were collected and counted with a hemocytometer. (B) Cells were cultured for 96 hours in complete cell medium in the presence of 10 μM PD173074. Cell viability was determined by MTT assay. (C and D) Dose-dependent effect of PD173074 on cell growth (48 hours). (C) Cells were grown in complete cell medium in the presence of the indicated doses of PD173074 for 48 hours and analyzed as described in (A). In (D), cells were cultured and analyzed as described in (B), and cell viability was determined by MTT assay. In (E), normal HUVECs and NHDFs were treated with PD173074, and cell viability was analyzed by MTT assay. Values represent the mean ± SE of at least three independent experiments. *P < .05 indicates that the values for PD173074-treated cells were less statistically significant than those for untreated cells. ns = not significant.*

Effect of PD173074 on the Anchorage-Independent Growth of Human Pancreatic Cancer Cells

To determine the growth-inhibitory efficacy of PD173074 on anchorage-independent growth, we analyzed pancreatic cancer cell lines in soft agar assays. Because of the duration and specific characteristics of this experimental setting, we used 1.0 μM PD173074 in this experiment, which is a concentration well below the IC_{50} concentration of pancreatic cancer cell lines. The well-differentiated human pancreatic cancer cell line Capan-1 did not grow in soft agar assays.

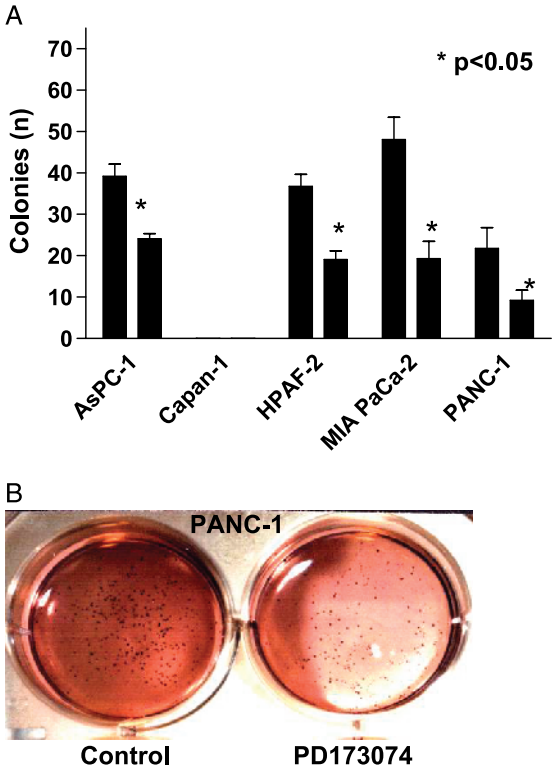

Figure 4. *Effect of PD173074 on anchorage-independent growth assays. (A) Pancreatic cancer cells (10^3–10^4) were seeded on a bottom layer dependent on individual cell growth rate. After 10 days of culture, the MTT reagent was added as described in the Materials and Methods section. Colonies with > 20 cells were counted. Values represent the mean ± SE of at least three independent experiments. *P < .05 indicates that values for PD173074-treated cells were statistically significantly different from those for untreated cells. (B) Representative culture of PANC-1 cells is shown. Untreated cells (left well) compared to PD173074-treated cells (right well) are shown after the MTT reagent has been added.*

In contrast, the growth of all four cell lines that grew in soft agar was markedly inhibited, similar to that seen in monolayer cultures, although lower concentrations were needed in anchorage-independent growth assays (Figure 4). In summary, the growth-inhibitory effect of equal concentrations of PD173074 was more pronounced in anchorage-independent growth assays than in monolayer cultures, where higher doses were needed for equal growth suppression (Figures 3 and 4).

Cell Cycle Arrest and Induction of Apoptosis after Treatment with PD173074

To analyze how PD173074 modulates the cell growth of pancreatic cancer cells *in vitro*, we analyzed whether PD173074 inhibited cell cycle progression or caused apoptosis by FACS analysis using hypotonic PI and annexin V cell stainings. Cell cycle progression was significantly inhibited in all pancreatic cancer cell lines tested, but a clear difference was observed with regard to the potency of inhibition (Table 1). AsPC-1 cells that expressed the highest levels of FGF-RI protein reacted with the most pronounced G_0/G_1–phase arrest (Table 1). Nevertheless, the HPAF-II cell line, in which FGF-RI was not detectable, also displayed cell cycle arrest, as seen as well for PANC-1 and MIA PaCa-2 cells (Table 1).

Apart from altering cell cycle progression, PD173047 therapy had a significant influence on apoptosis as it increased the rate of apoptosis in pancreatic cancer cells (Figure 5, *A* and *B*). Quantitative analysis of apoptotic rate with annexin V staining showed that PD173074 dose-dependently and time-dependently increased apoptosis (Figure 5, *A* and *B*). This effect was first detectable at a dose of 1.0 μM PD173074 in cells cultured for 48 hours. Similarly, 10 μM PD173074 resulted in an increase in apoptosis as early as 24 hours after the onset of treatment. The potency of induction was markedly different and more pronounced in cells with higher FGF-RI levels. Noteworthy also, the FGF-RI–negative cell line HAPF-II showed an increase in the rate of apoptosis (Figure 5, *A* and *B*). The dose and time dependencies of the effects of PD173074 on apoptosis overlapped with the corresponding effects of PD173074 on cell count and cell viability (Figure 3).

Therapeutic Efficacy of PD173074 In Vivo

For *in vivo* studies, we used a highly metastatic murine model for pancreatic cancer. One week after tumor induction, treatment was initiated, and 25 mg/kg per day PD173074 or an equal volume of solvent was injected intraperitoneally. Treatment was continued for 10 weeks. Only moderate side effects were seen in PD173074-treated animals, which

Table 1. Cell Cycle Phase Distribution of Pancreatic Cancer Cells Treated with PD173074.

		AsPC-1 (%)		Capan-1 (%)		HPAF-II (%)		MIA PaCa-2 (%)		PANC-1 (%)	
		Control	PD173074	Control	PD173074	Control	PD173074	Control	PD173074	Control	PD173074
48 hr	G_0/G_1	39	*59*	42	*59*	46	*55*	41	*58*	39	*67*
	S	43	32	37	29	35	29	48	31	34	18
	G_2/M	18	9	21	12	19	15	11	11	27	15
96 hr	G_0/G_1	43	*69*	39	*64*	47	*61*	38	*76*	42	*77*
	S	49	25	42	21	33	22	45	9	35	11
	G_2/M	8	6	19	15	20	17	17	15	23	12

Logarithmically growing pancreatic cancer cells were collected after 48 and 96 hours of treatment with 10 μM PD173074 and stained with PI, and DNA content was subjected to flow cytometry analysis. The percentage of cells in each cell cycle phase was determined by the analysis of DNA content histograms using ModFit LT software. Numbers in the G_0/G_1 phase that are presented in italics are statistically different from the corresponding control values ($P < .05$, Student's *t* test). Values from a representative experiment are presented, and similar results were obtained in at least two independent experiments.

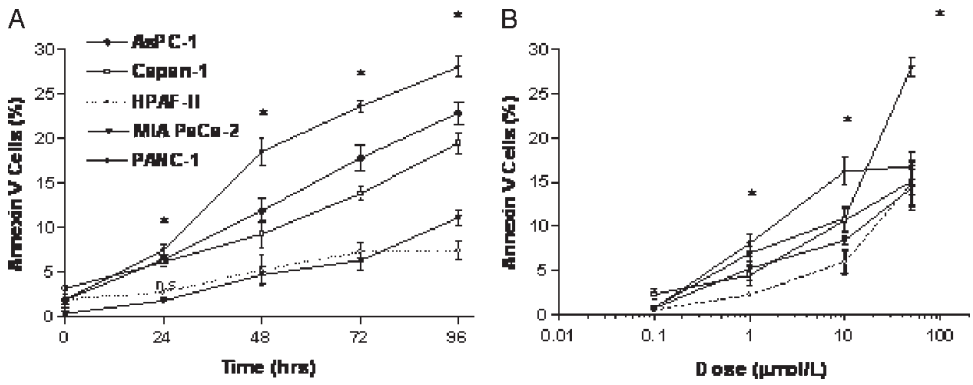

Figure 5. *Dose and time dependencies of PD173074-induced apoptosis in different human pancreatic cancer cell lines. Cells were treated with PD173074 (10 μM) for the indicated time (A) or cultured for 48 hours in the presence of the indicated doses of PD173074 (B). Cells were trypsinized and stained with annexin V and PI. Annexin V–positive and PI-negative cells were considered apoptotic. Values represent the mean ± SE of at least three independent experiments. *P < .05 indicates that for all cell lines studied, values for PD173074-treated cells were statistically significantly greater than those for untreated cells. ns = not significant.*

had a lower weight in both groups compared to the sham-treated animals.

PD173074 therapy resulted in significant tumor growth suppression (Table 2). Overall growth-suppressive efficiency was even more pronounced in the MIA PaCa-2 cell line than in the HPAF-II cell line. Local tumor infiltration into peripancreatic organs (e.g., stomach, liver, and spleen) was lower in the treated groups. Tumor metastasis was decreased in MIA PaCa-2 xenograft tumors on PD173074 treatment (Table 2), and a clear trend in HPAF-II tumors was seen, but this did not reach statistical significance in HPAF-II animals. Furthermore, the production of ascites in MIA PaCa-2 xenografted animals was reduced in the treated group.

In an attempt to further translate our *in vitro* results, we analyzed the apoptotic index in treated and untreated xenograft tumors (Figure 6, *A* and *B*). The quantification of apoptosis in xenografts paralleled *in vitro* findings, as PD173074 significantly ($P < .05$) increased the rate of apoptosis in both xenografted cell lines with a more pronounced effect on MIA PaCa-2 xenograft tumors (13.1 ± 3.9% *vs* 3.7 ± 1.8%) but also increased apoptosis in HPAF-II tumor xenografts (19.3 ± 6.2% *vs* 11.0 ± 4.1%).

Given the high potency of PD173074 for the simultaneous blockade of FGF-RI and VEGF-RII, the MVD of xenograft tumors was analyzed to test whether tumor-suppressive effects were also due to blocked angiogenesis (Figure 6, *C* and *D*). For specific identification, we stained tumor specimens from both groups with an anti-mouse CD31 antibody—a specific marker for blood vessel endothelium. MVD in MIA PaCa-2 xenograft tumors was reduced by > 30% on PD173074 treatment (41.9 ± 10.1 *vs* 63.4 ± 12.5), and a similar reduction was seen in HPAF-II xenografts as well (39.9 ± 12.8 *vs* 63.8 ± 13.2).

Table 2. Therapeutic Efficiency of PD173074 Treatment *In Vivo* Using a Highly Metastatic Orthotopic Murine Model for Pancreatic Cancer.

Tumor Parameters	MIA PaCa-2		HPAF-II	
	Sham	PD173074	Sham	PD173074
Tumor volume (cm^3)	1.57 ± 0.3	0.46 ± 1.5*	1.72 ± 0.3	0.90 ± 0.3*
Metastatic score	2.20 ± 0.5	0.90 ± 0.3*	1.20 ± 0.4	1.00 ± 0.3
Ascites volume (ml)	2.10 ± 0.7	0.60 ± 0.2*	1.50 ± 0.6	0.55 ± 0.3
Animal weight (g)	27.6 ± 1.6	21.3 ± 0.9*	29.5 ± 1.9	22.6 ± 1.1*

*$P < .05$, unpaired *t*-test.

Discussion

Pancreatic cancer is a devastating disease with only a few therapeutic options for the majority of patients, who have to be treated palliatively. Even those patients who undergo tumor resection often develop recurrent disease [42–44]. In a palliative therapeutic setting, radiation and chemotherapy offer—if at all—only marginal survival advantage [43,45–47]. Therefore, new treatment strategies and compounds are necessary to treat pancreatic cancer. Antiangiogenic therapy appears promising as it targets the nutritional support of tumor cells by inhibiting blood vessel formation [10,48,49]. Nevertheless, antiangiogenic therapy is adjunctive only and is usually given together with additional cytotoxic compounds [49]. PD173074 is a novel small molecule inhibitor, which blocks VEGF-RII and FGF-RI signaling [27,28]. By its dual affinity, PD173074 simultaneously exerts both the antiangiogenic and the antimitogenic activities of these growth factors, thus abrogating two crucial pathways in cancer growth and metastasis [41].

Because we have previously shown that mitogenic and active VEGF-RII is expressed in human pancreatic cancer cells *in vitro* and *in vivo*, we determined the expression of FGF-RI in various human cell lines [41]. FGF-RI expression was present in three of five pancreatic cancer cell lines, which could be stimulated with recombinant FGF-1. This mitogenic response induced by FGF-1 was completely revertible by PD173074. Additionally, a strong antiproliferative effect was observed in pancreatic cancer cells grown without further stimulation by growth factors. This effect was both dose-dependent and time-dependent in all cancer cell lines. Because higher doses of PD173074 inhibited the growth of all cancer cell lines (even those that did not express FGF-RI), it is likely that higher doses of PD173074 may also crossact through *nonspecific* inhibition of other growth factor receptors and tyrosine kinases. PD173074 demonstrated a selective

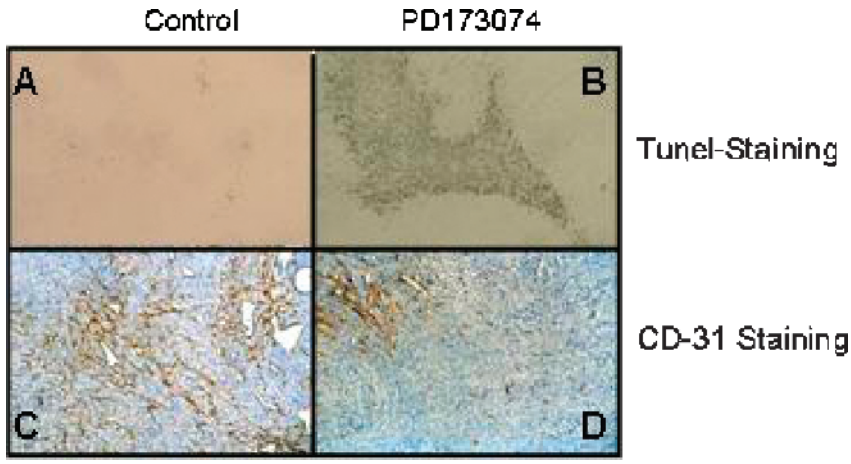

Figure 6. *Effect of PD173074 therapy on apoptosis and neoangiogenesis in an orthotopic pancreatic cancer xenograft model. Animals bearing orthotopic pancreatic xenograft tumors were treated with PD173074 (B and D) or with vehicle (A and C), as described in Materials and Methods section. Animals were sacrificed, and tissue samples of the primary tumor were fixed in formalin (A and B) and liquid nitrogen (C and D). Sections of 3 μm were stained using the TUNEL method (A and B). Nuclei positively stained for DNA breaks are seen as black dots (B). In (C) and (D), MVD analysis of frozen tissue sections stained with an anti-CD31 antibody is shown. In (C), a xenograft tumor of an animal with an untreated xenograft tumor is shown, whereas in (D), a xenograft tumor of an animal receiving PD173074 is shown.*

growth-inhibitory action toward HUVECs and normal human fibroblasts when compared with a panel of pancreatic cancer cells. In soft agar assays, a similar growth inhibition was observed, but the drug doses required were lower than those in monolayer cultures. Growth inhibition appeared to be mediated by altered cell cycle progression in the G_0/G_1 phase and by additional induction of apoptosis as determined by flow cytometry.

Because PD1730474 appears to inhibit growth *in vitro*, we tested the ability of this compound also *in vivo* using a highly metastatic orthotopic murine model for pancreatic cancer. In this study, we used a dose higher than that previously described for antiangiogenic studies with nontransformed endothelial cells [27]. In contrast, this study aimed to abrogate the mitogenesis of transformed cancer cells as well. In general, this dose regimen was well tolerated. Tumor growth in PD173074-treated animals was significantly reduced in both MIA PaCa-2 and HPAF-II animals. In the highly metastatic cell line MIA PaCa-2, there was also a lower incidence of metastatic tumor spread and a lower volume of ascites produced. A similar trend was seen in the dissemination score of HPAF-II–tumor bearing animals, but this observation did not reach statistical significance due to the relatively small sample size. The antitumor activity of PD173074 was most likely due to the simultaneous targeting of several cellular pathways affecting tumor cell proliferation, apoptosis, and tumor angiogenesis. In as much as the number of newly formed tumor blood vessels (MVD) may reflect the activity of tumor neoangiogenesis, we determined the number of blood vessels by staining them with endothelial-specific markers and found that PD173074 led to a significant reduction in tumor blood vessel formation. Clearly, reduction in the MVD itself is not specific for the antiangiogenic activity of a chemical compound because nonspecific tumor cell killing may also cause a reduction in blood vessel formation. Similarly treated animals showed a marked increase in apoptosis, similar to the effect seen *in vitro*.

The current study is the first study to have used high doses of PD173074 as a single compound and provides preclinical evidence that PD173074 tailored cancer therapy toward the simultaneous inhibition of angiogenesis, induction of apoptosis, and inhibition of tumor growth factor–mediated mitogenesis. By therapeutic unification of these pathways, a compound such as PD173074 may represent a new and promising treatment option for patients suffering from pancreatic cancer.

References

[1] Carmeliet P (2003). Angiogenesis in health and disease. *Nat Med* **9**, 653–660.
[2] Hanahan D (1997). Signaling vascular morphogenesis and maintenance. *Science* **277**, 48–50.
[3] Jemal A, Murray T, Ward E, Samuels A, Tiwari RC, Ghafoor A, Feuer EJ, and Thun MJ (2005). Cancer statistics, 2005. *CA Cancer J Clin* **55**, 10–30.
[4] Lowenfels AB, Sullivan T, Fiorianti J, and Maisonneuve P (2005). The epidemiology and impact of pancreatic diseases in the United States. *Curr Gastroenterol Rep* **7**, 90–95.
[5] Riela A, Zinsmeister AR, Melton LJ III, Weiland LH, and DiMagno EP (1992). Increasing incidence of pancreatic cancer among women in Olmsted County, Minnesota, 1940 through 1988. *Mayo Clin Proc* **67**, 839–845.
[6] DiMagno EP, Reber HA, and Tempero MA (1999). AGA technical review on the epidemiology, diagnosis, and treatment of pancreatic ductal adenocarcinoma. *Gastroenterolgy* **117**, 1464–1484.
[7] von Marschall Z, Cramer T, Hocker M, Burde R, Plath T, Schirner M, Heidenreich R, Breier G, Riecken EO, Wiedenmann B, et al. (2000). *De novo* expression of vascular endothelial growth factor in human pancreatic cancer: evidence for an autocrine mitogenic loop. *Gastroenterology* **119**, 1358–1372.
[8] Buchler P, Reber HA, Ullrich A, Shiroiki M, Roth M, Buchler MW, Lavey RS, Friess H, and Hines OJ (2003). Pancreatic cancer growth is inhibited by blockade of VEGF-RII. *Surgery* **134**, 772–782.
[9] Buchler P, Reber HA, Buchler M, Shrinkante S, Buchler MW, Friess H, Semenza GL, and Hines OJ (2003). Hypoxia-inducible factor 1 regulates vascular endothelial growth factor expression in human pancreatic cancer. *Pancreas* **26**, 56–64.
[10] Bergers G, Javaherian K, Lo KM, Folkman J, and Hanahan D (1999). Effects of angiogenesis inhibitors on multistage carcinogenesis in mice. *Science* **284**, 808–812.
[11] Yancopoulos GD, Klagsbrun M, and Folkman J (1998). Vasculogenesis,

angiogenesis, and growth factors: ephrins enter the fray at the border [comment]. *Cell* **93**, 661–664.
[12] Folkman J (1997). Angiogenesis and angiogenesis inhibition: an overview. *EXS* **79**, 1–8.
[13] Plate KH, Breier G, Weich HA, and Risau W (1992). Vascular endothelial growth factor is a potential tumour angiogenesis factor in human gliomas *in vivo*. *Nature* **359** (6398), 845–848.
[14] Itakura J, Ishiwata T, Friess H, Fujii H, Matsumoto Y, Buchler MW, and Korc M (1997). Enhanced expression of vascular endothelial growth factor in human pancreatic cancer correlates with local disease progression. *Clin Cancer Res* **3**, 1309–1316.
[15] Yamanaka Y, Friess H, Buchler M, Beger HG, Uchida E, Onda M, Kobrin MS, and Korc M (1993). Overexpression of acidic and basic fibroblast growth factors in human pancreatic cancer correlates with advanced tumor stage. *Cancer Res* **53**, 5289–5296.
[16] Soker S, Takashima S, Miao HQ, Neufeld G, and Klagsbrun M (1998). Neuropilin-1 is expressed by endothelial and tumor cells as an isoform-specific receptor for vascular endothelial growth factor. *Cell* **92**, 735–745.
[17] Millauer B, Wizigmann-Voos S, Schnürch H, Martinez R, Møller NP, Risau W, and Ullrich A (1993). High affinity VEGF binding and developmental expression suggest Flk-1 as a major regulator of vasculogenesis and angiogenesis. *Cell* **72** (6), 835–846.
[18] De Vries C, Escobedo JA, Ueno H, Houck K, Ferrara N, and Williams LT (1992). The fms-like tyrosine kinase, a receptor for vascular endothelial growth factor. *Science* **255**, 989–991.
[19] Terman BI, Dougher-Vermazen M, Carrion ME, Dimitrov D, Armellino DC, Gospodarowicz D, and Bohlen P (1992). Identification of the KDR tyrosine kinase as a receptor for vascular endothelial cell growth factor. *Biochem Biophys Res Commun* **187**, 1579–1586.
[20] Chen H, Chedotal A, He Z, Goodman CS, and Tessier-Lavigne M (1997). Neuropilin-2, a novel member of the neuropilin family, is a high affinity receptor for the semaphorins Sema E and Sema IV but not Sema III [published erratum appears in *Neuron* 1997 Sep;19(3):559]. *Neuron* **19**, 547–559.
[21] Lee PL, Johnson DE, Cousens LS, Fried VA, and Williams LT (1989). Purification and complementary DNA cloning of a receptor for basic fibroblast growth factor. *Science* **245**, 57–60.
[22] Dvorak HF, Detmar M, Claffey KP, Nagy JA, Van De WL, and Senger DR (1995). Vascular permeability factor/vascular endothelial growth factor: an important mediator of angiogenesis in malignancy and inflammation. *Int Arch Allergy Immunol* **107**, 233–235.
[23] Yoshiji H, Harris SR, and Thorgeirsson UP (1997). Vascular endothelial growth factor is essential for initial but not continued *in vivo* growth of human breast carcinoma cells. *Cancer Res* **57**, 3924–3928.
[24] Wagner M, Kleeff J, Friess H, Buchler MW, and Korc M (1999). Enhanced expression of the type II transforming growth factor-beta receptor is associated with decreased survival in human pancreatic cancer. *Pancreas* **19**, 370–376.
[25] Milanini J, Vinals F, Pouyssegur J, and Pages G (1998). p42/p44 MAP kinase module plays a key role in the transcriptional regulation of the vascular endothelial growth factor gene in fibroblasts. *J Biol Chem* **273**, 18165–18172.
[26] Kroll J and Waltenberger J (1997). The vascular endothelial growth factor receptor KDR activates multiple signal transduction pathways in porcine aortic endothelial cells. *J Biol Chem* **272**, 32521–32527.
[27] Mohammadi M, Froum S, Hamby JM, Schroeder MC, Panek RL, Lu GH, Eliseenkova AV, Green D, Schlessinger J, and Hubbard SR (1998). Crystal structure of an angiogenesis inhibitor bound to the FGF receptor tyrosine kinase domain. *EMBO J* **17**, 5896–5904.
[28] Mohammadi M, McMahon G, Sun L, Tang C, Hirth P, Yeh BK, Hubbard SR, and Schlessinger J (1997). Structures of the tyrosine kinase domain of fibroblast growth factor receptor in complex with inhibitors. *Science* **276**, 955–960.
[29] Chen WH, Horosezeicz JS, Leong SS, Shimano T, Penetrante R, Sanders WH, Berjian R, Douglass HO, Martin EW, and Chu TM (1982). Human pancreatic adenocarcinoma: *in vitro* and *in vivo* morphology of a new tumor cell line established from ascites. *In Vitro* **18**, 24–34.
[30] Ding X, Flatt PR, Permert J, and Adrian TE (1998). Pancreatic cancer cells selectively stimulate islet β cells to secrete amylin. *Gastroenterology* **114**, 130–138.
[31] Yunis AA, Arimura GK, and Russin DJ (1977). Human pancreatic carcinoma (MIA PaCa-2) in continuous culture: sensitive to asparaginase. *Int J Cancer* **19**, 128–135.
[32] Kyriazis AP, Kyriazis AA, Scarpelli DG, Fogh J, Sambasiva Rao JF, and Lepera R (1982). Human pancreatic adenocarcinoma line Capan-1 in tissue culture and the nude mice. *Am J Pathol* **106**, 250–260.
[33] Lieber M, Mazzetta J, Nelson-Rees W, Kaplan M, and Todaro G (1975). Establishment of a continuous tumor-cell line (PANC-1) form a human carcinoma of the exocrine pancreas. *Int J Cancer* **15**, 741–747.
[34] Mosmann T (1983). Rapid colorimetric assay for cellular growth and survival: application to proliferation and cytotoxicity assays. *J Immunol Methods* **65**, 55–63.
[35] Buchler P, Reber HA, Lavey RS, Tomlinson J, Buchler MW, Friess H, and Hines OJ (2004). Tumor hypoxia correlates with metastatic tumor growth of pancreatic cancer in an orthotopic murine model. *J Surg Res* **120**, 295–303.
[36] Buchler P, Reber HA, Buchler MW, Friess H, Lavey RS, and Hines OJ (2004). Antiangiogenic activity of genistein in pancreatic carcinoma cells is mediated by the inhibition of hypoxia-inducible factor-1 and the down-regulation of VEGF gene expression. *Cancer* **100**, 201–210.
[37] Vermeulen PB, Gasparini G, Fox SB, Toi M, Martin L, McCulloch P, Pezzella F, Viale G, Weidner N, Harris AL, et al. (1996). Quantification of angiogenesis in solid human tumours: an international consensus on the methodology and criteria of evaluation. *Eur J Cancer* **32A**, 2474–2484.
[38] Weidner N and Folkman J (1996). Tumoral vascularity as a prognostic factor in cancer. *Important Adv Oncol*, 167–190.
[39] Hasan J, Byers R, and Jayson GC (2002). Intra-tumoural microvessel density in human solid tumours. *Br J Cancer* **86**, 1566–1577.
[40] Vermeulen PB, Gasparini G, Fox SB, Colpaert C, Marson LP, Gion M, Belien JA, de Waal RM, Van Marck E, Magnani E, et al. (2002). Second international consensus on the methodology and criteria of evaluation of angiogenesis quantification in solid human tumours. *Eur J Cancer* **38**, 1564–1579.
[41] Buchler P, Reber HA, Buchler MW, Friess H, and Hines OJ (2002). VEGF-RII influences the prognosis of pancreatic cancer. *Ann Surg* **236**, 738–749.
[42] Alexakis N, Halloran C, Raraty M, Ghaneh P, Sutton R, and Neoptolemos JP (2004). Current standards of surgery for pancreatic cancer. *Br J Surg* **91,** 1410–1427.
[43] Neoptolemos JP, Stocken DD, Friess H, Bassi C, Dunn JA, Hickey H, Beger H, Fernandez-Cruz L, Dervenis C, Lacaine F, et al. (2004). A randomized trial of chemoradiotherapy and chemotherapy after resection of pancreatic cancer. *N Engl J Med* **350**, 1200–1210.
[44] Yeo CJ and Cameron JL (2000). The treatment of pancreatic cancer. *Ann Chir Gynaecol* **89**, 225–233.
[45] Abrams RA, Grochow LB, Chakravarthy A, Sohn TA, Zahurak ML, Haulk TL, Ord S, Hruban RH, Lillemoe KD, Pitt HA, et al. (1999). Intensified adjuvant therapy for pancreatic and periampullary adenocarcinoma: survival results and observations regarding patterns of failure, radiotherapy dose and CA19-9 levels. *Int J Radiat Oncol Biol Phys* **44**, 1039–1046.
[46] Neoptolemos JP, Dunn JA, Stocken DD, Almond J, Link K, Beger H, Bassi C, Falconi M, Pederzoli P, Dervenis C, et al. (2001). Adjuvant chemoradiotherapy and chemotherapy in resectable pancreatic cancer: a randomised controlled trial. *Lancet* **358**, 1576–1585.
[47] Ihse I, Andersson R, Axelson J, and Hansson L (1998). Combination therapy in oncology (multimodal treatment) in pancreatic tumors. *Chirurg* **69**, 366–370.
[48] Skobe M, Rockwell P, Goldstein N, Vosseler S, and Fusenig NE (1997). Halting angiogenesis suppresses carcinoma cell invasion. *Nat Med*, 1222–1227.
[49] Nukui Y, Picozzi VJ, and Traverso LW (2000). Interferon-based adjuvant chemoradiation therapy improves survival after pancreaticoduodenectomy for pancreatic adenocarcinoma. *Am J Surg* **179**, 367–371.